IGF Workshop "Fracture and Structural Integrity"

Mechanical Qualification of the Hybrid Metal Extrusion & Bonding (HYB) Process for Butt Welding of 4 mm Plates of AA6082-T6

Filippo Berto[a],*, Lise Sandnes[a], Øystein Grong[a,b], Paolo Ferro[c]

[a]Norwegian University of Science and Technology, Department of Mechanical and Industrial Enginering, Richard Birkelands vei 2b, Trondheim 7491, Norway
[b]HyBond AS, Alfred Getz vei 2, 7491 Trondheim, Norway
[c]University of Padua, Department of Management and Engineering, Stradella San Nicola 3, Vicenza, Italy

Abstract

Hybrid Metal Extrusion & Bonding (HYB) is a novel solid state joining technique mainly developed for aluminum alloys. By the use of filler material addition and plastic deformation sound joints can be produced at operational temperatures below 400°C. Here, we present the results from an exploratory investigation of the mechanical integrity of a 4 mm AA6082-T6 HYB joint, covering both hardness, tensile and Charpy V-notch testing of different weld zones. The joint is found to be free from defects like pores, internal cavities and kissing-bonds. Still, a soft heat affected zone (HAZ) is present. The joint yield strength is 54 % of the base material, while the corresponding joint efficiency is 66 %. Therefore, there is room for further optimization of the HYB process. This work is now in progress.

Keywords: Welding; Solid State; Hybrid Metal Extrusion & Bonding (HYB); Aluminum Alloys; Mechanical Properties.

1. Introduction

The unique physical and mechanical properties of aluminum alloys, as the precipitation hardened Al-Mg-Si alloys, makes them attractive for a wide range of applications as structural components and welded assemblies. In particular, there is an increased use of aluminum alloys within the automotive industry as a result of the growing demand for

* Corresponding author. Tel.: +47 485 00 575; fax: +47 485 00 576.
  E-mail address: Filippo.Berto@ntnu.no

more fuel efficient and lightweight vehicles. In fact, a full aluminum car body design permits weight savings up to 30-40%, as stated by Hirsch (2011). However, within the automotive industry welding is often required as part of the fabrication process, and even though the Al-Mg-Si alloys are readily weldable, a variety of weld defects may occur. For instance, the excessive heat generated through traditional welding processes makes them vulnerable to heat affected zone (HAZ) softening due to reversion of the hardening precipitates which form during artificial ageing (see Hatch (1984)). Moreover, the material melting occurring during fusion welding makes the weld susceptible to pore formation, hot and liquation cracking as well as bonding defects causing additional degradation of the joint. (e.g. see Davis (1993) or Grong (1997)). Therefore, solid state joining offers several advantages compared to traditional fusion welding when it comes to structural and mechnaical integrity of the weldments.

Over the years a variety of solid state joining processes have been developed, and among the more recent ones is friction stir (FS) welding. Since its entery in 1991 the FSW process has continuously evolved due to the systematic research and development, including parameter optimization and new tool design. This has brought FSW to the forefront of aluminum welding technology (see Threadgill et al. (2009) and Nandan et al. (2008)). Although FSW is approaching its ultimate technology maturity level, the frictional heat generated through the process is still large enough to cause HAZ softening. In addition, strict profile tolerances are required, as lack of filler material addition may result in insufficient material feeding and consequently to undercuts and internal defects in the joint. These fundamental limitations need to be overcome in the future by new process developments.

Despite its recent introduction, it is believed that the Hybrid Metal Extrusion & Bonding (HYB) process has the potential to comepete with commonplace welding techniques in the future when it has been further developed and optimized. By the use of filler material addition and plastic deformation sound joints can be produces in solid state employing this technique (see Sandnes et al. (2018)). At the same time, the filler material addition makes the process more flexible and less voulnerable to undercuts and weld defects compared to conventional solid state joining processes. Therefore, in order to illuminate the potential of the HYB process, we aim to put it to the test in its pressent stage of development. This will be done by characterizing a 4 mm AA6082-T6 butt weld based on hardness measuremernts, tensile testing and Charpy V-nocth testing of different regions across the weld zones.

2. Current Status of the HYB Technology

The HYB PinPoint extruder is based on the principles of continuous extrusion. The current version of the extruder is built around a 10 mm diameter rotating pin, provided with an extrusion head with a set of moving dies through which the aluminum is allowed to flow. This is shown by the drawing in Fig. 1(a). When the pin is rotating, the inner extrusion chamber with three moving walls will drag the filler wire both into and through the extruder due to the imposed friction grip. At the same time, it is kept in place inside the chamber by the stationary steel housing constituting the fourth wall. The aluminum is then forced to flow against the abutment blocking the extrusion chamber and subsequently (owing to the pressure build-up) continuously extruded through the moving dies in the extruder head.
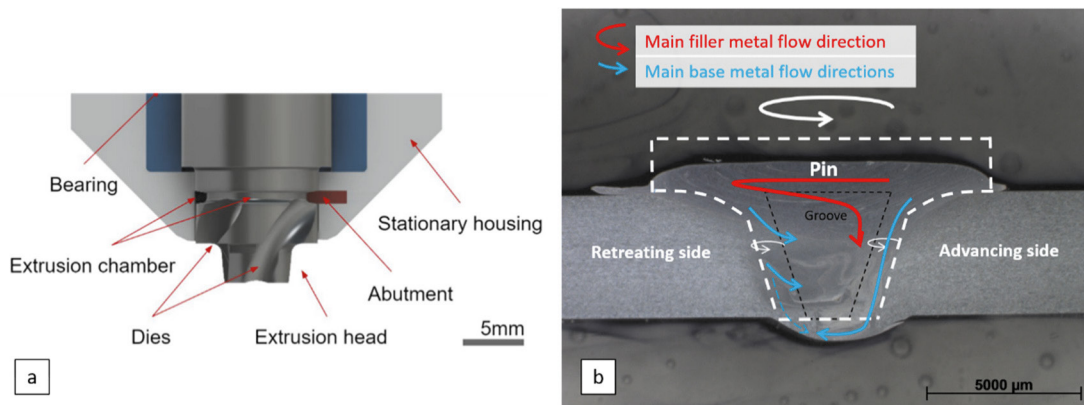

Fig. 1. (a) Schematic illustration of the main components of the HYB PinPoint Extruder; (b) Cross sectional view of a HYB butt joint. Included is also a schematic illustration of the material flow pattern during joining.

In a real joining situation, the extruder head is clamped against the two aluminum plates to be joined. The plates are separated from each other so that an I-groove is formed in-between. The pin diameter is slightly larger than the groove width to ensure contact between the sidewalls of the groove and the pin. Analogue to that in FSW, the side of the joint where the tool rotation is the same as the welding direction is referred to as the advancing side (AS), whereas the opposite side is referred to as the retreating side (RS). During pin rotation, some of the base material along with the oxide layer on the groove sidewalls will be dragged around by the motion of the pin. Hence, the surface oxide tends to mix with the filler material as it flows downwards into the groove and consolidates behind the pin. The base and filler materials flow during processing are schematically illustrated in Fig. 1(b). Typically, the temperature in the groove between the two base plates to be joined is between 350 and 400°C, which is below the conventional operating temperature for FSW, as reported by Frigaard et al. (2001).

3. Experimental

3.1. Materials and Welding Conditions

In the present welding trial, 4 mm rolled plates of aluminum alloy 6082-T6 were used as base material. These were obtained from an external supplier. The dimensions of the plates prior to welding were 120 mm x 60 mm. The filler wire was a Ø1.2 mm wire of the AA6082-T4 type produced by HyBond AS. The wire was made from a DC cast billet, which then was homogenized, hot extruded, cold drawn and shaved down to final dimension. The chemical compositions of the base and filler materials are summarized in Table 1. The HYB single-pass butt joining of the plates was carried out by HyBond AS, using an I-groove with 3 mm root opening and the following welding parameters: pin rotation of 400 RPM, travel speed of 6 mm/s, wire feed rate of 142 mm/s. The gross heat input during welding was 0.34 kJ/mm.

Table 1. Chemical composition (wt. %) of the base and filler materials (BM and FM).

	Si	Mg	Cu	Fe	Mn	Cr	Zn	Ti	Zr	B	Other	Al
Base material	0.9	0.80	0.06	0.45	0.42	0.02	0.05	0.02	-	-	0.03	Balance
Filler material	1.11	0.61	0.002	0.20	0.51	0.14	-	0.043	0.13	0.006	0.029	Balance

3.2. Mechanical Testing

Transverse samples were cut from the HYB welded plates. The tensile and Charpy V-notch (CVN) specimens were located in different regions of the weld relative to the center-line. They were subsequently flush-machined to remove the contribution from the weld reinforcement. Details of the specimen location and number of specimens being tested can be found in Fig. 2. In addition, three separate sets of tensile and CVN specimens sampling the unaffected base material were prepared from a separate base plate. The subsize tensile specimens were prepared in accordance with ASTM standard E8/E8M-16a, with a thickness of 4 mm (corresponding to the plate thickness). Tensile testing was carried out at room temperature using an Instron hydraulic test machine (50 kN load cell) with a fixed cross-head speed of 1.5 mm/min. The applied gauge length was 25 mm. Similarly, the subsize CVN specimens were prepared in accordance with ASTM standard E23-12c (type A) with a thickness of 4 mm (corresponding to the plate thickness). The CVN testing was carried out at room temperature, using a Zwick impact testing machine with a total impact energy absorption capacity of 450 J.

The specimens used for microstructural analysis and hardness testing were prepared according to standard sample preparation procedures. To reveal the micro- and macrostructure of the joint, the specimen was immersed in an alkaline sodium hydroxide solution (1g NaOH + 100 ml H_2O) for 3-4 min. The macro and microstructure of the weld were analyzed using a Leica DMLB light microscope and an Alicona Confocal Microscope. Transverse Vickers hardness measurements HV (1 kg load) were performed in accordance to the ASTM standard E92-16, both along the horizontal and vertical mid-sections of the joint (see Fig. 2(b)) using a Mitutoyo Micro Vickers Hardness Testing Machine (HM-200 Series). In total, three test series were carried out for each test line. The base material hardness was established from ten individual measurements being randomly taken on one separate base material specimen. Finally, the fracture surfaces of broken tensile and CVN specimens were examined in a Quanta FEG 450 scanning electron microscope (SEM).
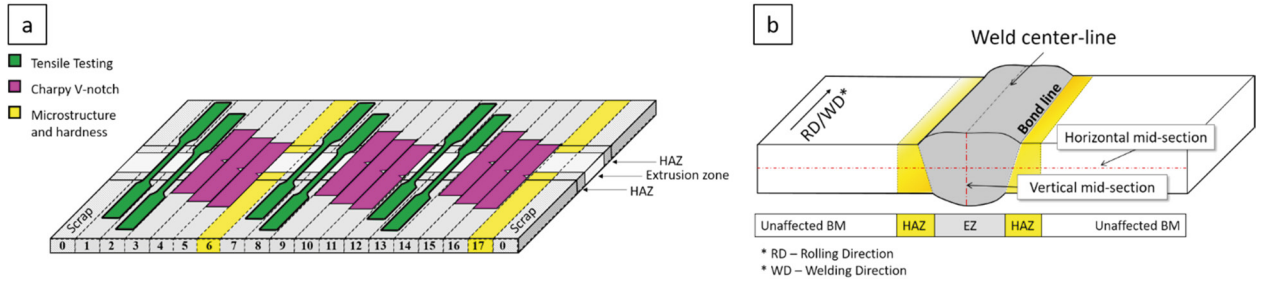
Fig. 2. (a) Schematic illustration of sample location relative to the weld center-line. Also the number of specimens tested is indicated; (b) Schematic illustration of different weld zones in the HYB butt joint. BM: base material, BL: Bond line, HAZ: Heat affected zone, EZ: extrusion zone.

4. Results

4.1. Weld Macrostructure and Hardness Profile

The measured hardness profile along the horizontal mid-section of the HYB joint is presented in Fig. 3(a). Moreover, Fig. 3(b) shows an overview of the different weld zones, from which the FM and BM flow patterns in the groove also can be seen. Note that each hardness point represents the arithmetic mean of three individual measurements. The vertical dotted line in Fig. 3(a) represents the hardness of the unaffected BM, measured to be 111 HV with a standard deviation of 2.2. The minimum hardness is found on the advancing side of the joint, yielding a value of 66 HV approximately 3 mm from the center-line. The total width of the HAZ is estimated to be 25 mm. The hardness measurements along the vertical mid-section revealed that the hardness was highest in the top region, where it reached a value of 93 HV. The hardness then dropped monotonically with increasing depths below the plate surface, finally approaching its lowest value of 51 HV at the weld toe.
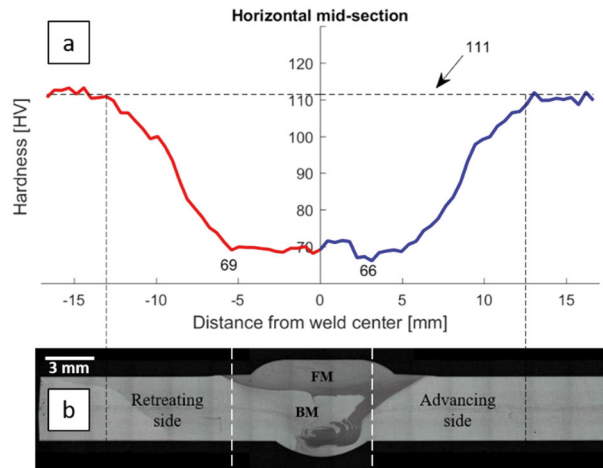

Fig. 3. (a) Measured hardness profile along the horizontal mid-section of the HYB joint; (b) Optical micrograph showing the macrostructure of the HYB joint in the transverse direction.

4.2. Tensile Properties

The measured tensile properties of the HYB joint are graphically presented in Fig. 4. It is evident that the welded specimens (EZ and HAZ) have significantly lower tensile properties compared to the base material. However, there is apparently no difference between the EZ and the HAZ. The weld yield strength (indicated by the bars to the right

in Fig. 4(a)) amounts to 54% of the BM yield strength, while the corresponding joint efficiency (i.e. $\sigma_{UTS,HAZ}/\sigma_{UTS,BM}$ ratio) is higher reaching a value of 66%. The elongation at fracture of the different weld zones is presented in Fig. 4(b). Owing to the necking effect caused by the HAZ softening the measured elongation of the welded specimens is seen to be significantly lower than that of the base material. Another consequence of the HAZ softening is also that fracture always occurs in the HAZ on the advancing side of the joint regardless of the sample location (i.e. whether it is located on the advancing side or not). This is in good agreement with the results from the transverse hardness measurements in Fig. 3.
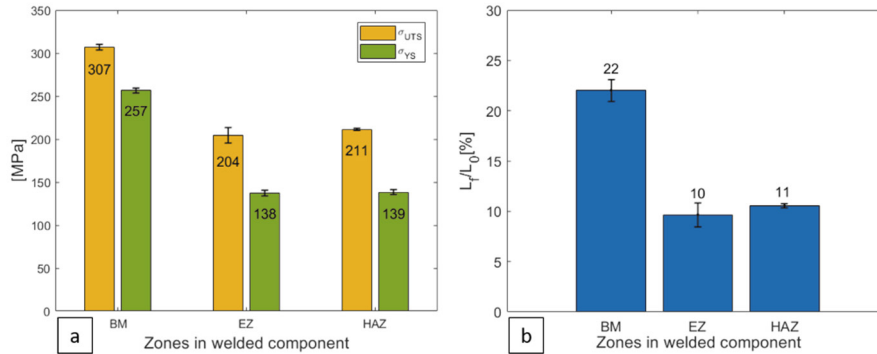

Fig. 4. Average tensile properties for specimens sampling different weld zones. (a) Offset yield strength and ultimate tensile strength; (b) Elongation at fracture. The error bars in the graphs represent the standard deviation of three individual measurements.

4.3. Energy Absorption

The joint response to very high strain rates ($>10^3$ s^{-1}) was determined using CVN testing. The measured energy absorption (per unit area) for different weld regions is shown in Fig. 5. The base material displays a relatively low initial toughness, whereas all welded specimens show an increase in impact toughness relative to the base material. The highest energy absorption is found for the EZ specimens, which is almost three times larger than that of the base material. No difference is observed between the bond line (BL) and the HAZ energy absorption.
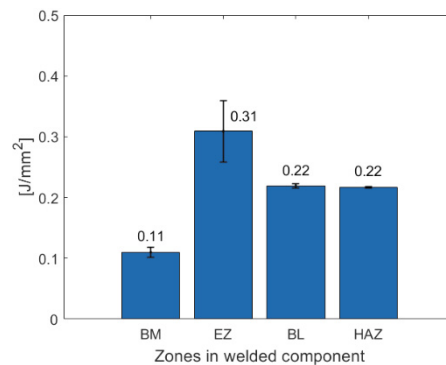

Fig. 5. Measured energy absorption for CVN specimens sampling different weld zones: base material (BM), extrusion zone (EZ), bond line (BL) and heat affected zone (HAZ). The error bars in the graph represent the standard deviation of three individual measurements.

4.4. Microscopic Analysis

The microstructure of the HYB joint is shown in Fig. 6(a). Obviously, the microstructure changes across the bond line, and the filler material reveals much finer grains compared to the HAZ. Close to the bond line strongly elongated and heavily deformed grains are visible. Fig. 6(b) shows a representative image of the fracture surface of a broken welded tensile specimen. Extensive dimple formation is observed being characteristic of a ductile fracture. As a matter

of fact, all tensile and CVN specimens examined in SEM revealed the same fracture mode, thereby excluding possible kissing bond formation. This means that full metallic bonding is achieved in the groove between the FM and BM under the prevailing circumstances.
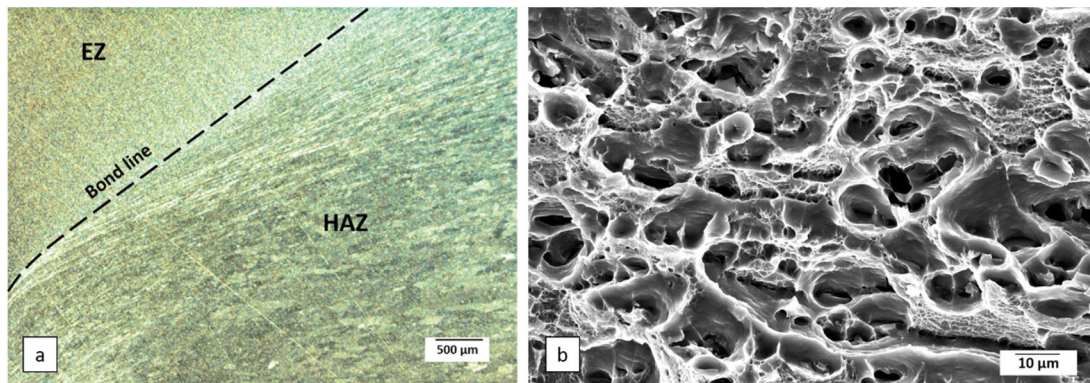

Fig. 6. (a) Optical micrograph showing the changes in microstructure across the bond line between the base and filler materials; (b) Representative SEM fractograph of a selected broken tensile specimen sampling the EZ.

5. Discussion

In order to evaluate the HYB joint mechanical performance the experimental results are collated to comparable values reported for conventional welding technologies such as gas metal arc (GMA) welding and friction stir (FS) welding. Among others, the transverse hardness profiles and tensile properties of AA6082-T6 GMA and FS welded plates have been determined by Moreira et al. (2007), Moreira et al. (2009) and by Ericsson and Sandström (2003). In the work of Moreira et al. 3 mm thick rolled plates were used as base material, whereas in the work of Ericsson and Sandström 4 mm thick extruded profiles were used. In these reports, the total width of the HAZ in the GMA welds varied between 35 mm and 50 mm. For the FS welds these values are significantly lower, varying between 20 mm and 25 mm, depending on the applied welding speed. The corresponding value for the HYB joint is 25 mm (revisit Fig. 3(a)). To completely eliminate problems related to HAZ softening in Al-Mg-Si weldments, the operational temperature needs to be kept below about 250°C, as shown by Myhr et al. (2004). This is physically feasible and within the reach of what is possible using the HYB process as demonstrated by Aakenes (2013) and Aakenes et al. (2014).

Moving on to the tensile properties, the GMA welds have a yield strength corresponding to about 50% of the base material and a joint efficiency of 70%. On the other hand, the FS welds reaches a yield strength of 52% with a joint efficiency of about 80%. In comparison, the HYB joint yield strength is 54%, while the joint efficiency is 66%. This indicates that the mechanical performance of the HYB joint is within the range of that reported for conventional welding technologies such as GMAW and FSW.

6. Conclusions

Here, we present the successful HYB joining of 4 mm AA6082-T6 rolled plates. The joints are free from defects like pores and internal cavities. Full metallic bonding is achieved between the filler material and the base material in the groove, as demonstrated by both tensile testing and Charpy V-notch (CVN) testing. Transverse hardness testing of the HYB joint disclosed evidence of significant HAZ softening, reaching a total HAZ width of 25 mm. This reduces both the yield strength and the efficiency of the joint to values well below that of the base material (54% and 66%, respectively). In contrast, the HAZ softening appears to have a positive effect on the CVN impact toughness, which is about three times larger for the welded specimens. However, the increase in toughness is mainly believed to reflect the low initial base material toughness, which subsequently becomes healed by the HAZ softening. Moreover, to get an indication of the HYB joint mechanical performance a comparison with similar GMA and FS welds has also been made. This shows that the HYB joint mechanical properties are slightly better than the properties reported for similar

GMA welds, but do not fully match those of sound FS welds. Therefore, there is still a potential for further optimization of the HYB process in order to bring the process to the forefront of aluminum welding technology.

References

Aakenes, U.R., 2013. Industrialising of the Hybrid Metal Extrusion & Bonding (HYB) Method–From Prototype Towards Commercial Process [dissertation]. Norwegian University of Science and Technology, Trondheim, Norway.

Aakenes, U.R., et al., 2014. Application of the Hybrid Metal Extrusion & Bonding (HYB) Method for Joining of AA6082-T6 Base Material. Materials Science Forum 794, 339-344.

Davis, J.R., 1993. Aluminum and aluminum alloys. ASM international,

Materials Park, OH.

Ericsson, M., Sandström, R., 2003. Influence of welding speed on the fatigue of friction stir welds, and comparison with MIG and TIG. International Journal of Fatigue 25, 1379-1387.

Frigaard, Ø., et al., 2001. A process model for friction stir welding of age hardening aluminum alloys. Metallurgical and Materials Transactions A 32, 1189-1200.

Grong, Ø., 1997. Metallurgical modelling of welding. Institute of Materials, Cambridge (UK).

Hatch, J.E., 1984. Aluminum - Properties and Physical Metallurgy. American Society for Metals, Materials Park, OH.

Hirsch, J., 2011. Aluminium in innovative light-weight car design. Materials Transactions 52, 818-824.

Moreira, P.M.G.P., et al., 2007. Fatigue behaviour of FSW and MIG weldments for two aluminium alloys. Theoretical and Applied Fracture Mechanics 48, 169-177.

Moreira, P.M.G.P., et al., 2009. Mechanical and metallurgical characterization of friction stir welding joints of AA6061-T6 with AA6082-T6. Materials & Design 30, 180-187.

Myhr, O., et al., 2004. Modelling of the microstructure and strength evolution in Al–Mg–Si alloys during multistage thermal processing. Acta Materialia 52, 4997-5008.

Nandan, R., et al., 2008. Recent advances in friction-stir welding – Process, weldment structure and properties. Progress in Materials Science 53, 980-1023.

Sandnes, L., et al., 2018. Exploring the Hybrid Metal Extrusion & Bonding (HYB) Process for Butt Welding of Al-Mg-Si Alloys. The International Journal of Advanced Manufacturing Technology.

Threadgill, P., et al., 2009. Friction stir welding of aluminium alloys. International Materials Reviews 54, 49-93.